Chemical Engineering Journal 110 (2005) 19–29

Chemical Engineering Journal

www.elsevier.com/locate/cej

Numerical study on particle size distribution in the process of preparing ultrafine particles by reactive precipitation

Jin Zhao, Jianwen Zhang *, Ming Xu, Jianfeng Chen

College of Chemical Engineering, Beijing University of Chemical Technology, Research Center of the Ministry of Education for High Gravity Engineering and Technology, Beijing 100029, China

Received 15 October 2004; received in revised form 15 April 2005; accepted 19 April 2005

Abstract

Based on the population balance and mass balance in a reactive precipitation process, a numerical simulation model was developed to predict the particle size distribution (PSD) in the reactive precipitation process. The precipitation system of $BaCl_2$ with Na_2SO_4 to prepare $BaSO_4$ in aqueous solution was adopted to obtain ultrafine particles in a stirred precipitation reactor and the particle size distribution and the morphology of the particle were observed under transmission electron microscope. It was illustrated by the experimental observation of the micrographs of $BaSO_4$ particles obtained that apparent agglomeration occurred between the particles, which phenomenon must be taken into consideration in PSD modeling. The population balance equation was calculated by discretization method to obtain particle number and particle size distribution. By implementing the model, the reactive precipitation process in a batch reactor including reaction, nucleation, growth and agglomeration was simulated. The simulation results were validated by the experimental data of $BaSO_4$ precipitation. Further analysis was endeavored to explore the effects of some important factors such as the supersaturation degree and agglomeration on the evolution of the volume-based characteristic particle size and the variance of volume-based characteristic size of the particles. It was depicted that particle size and particle size distribution are controlled by the supersaturation degree and agglomeration between the particles. Stemming from the analysis in the context, the disciplinarian of the influences of these factors and the method for controlling particle size distribution were presented for the reactive precipitation process.

Keywords: Reactive precipitation; Agglomeration; Particle size distribution; Numerical simulation

1. Introduction

Crystallization from solution is one of the oldest and most economical industrial separation and purification processes. It is applied as a large scale batch or continuous process for the production of inorganic (e.g. potassium chloride, ammonium sulphate) and organic (e.g. adipic acid) materials. On a small scale it is often applied as a batch operation to produce high purity and high value-added pharmaceuticals or fine chemicals. Reactive precipitation is an important branch of crystallizations used for producing a solid phase of high purity from a fluid phase at low cost.

For practical use, the effective control of precipitation is required since the quality of the product has important effect on the solid–liquid separation and the properties of the powders, such as the specific surface area, the crystal morphology, the crystal size and the purity. In other words, the performance of a crystallizer is assessed not only by the yield of the product but also the quality of the product. For various precipitation applications, the particle size distribution (PSD) is of primary importance to the product quality. The requirements on the product such as the ability to flow or the dissolution rate of the produced particles can be directly related to the PSD [1]. Furthermore, the PSD directly influences the performance of the downstream separation units. From the view of the industrial application, the refined control of the PSD, and notably the improvement on process reproducibility, are the key concerns. During the precipitation

* Corresponding author. Tel.: +86 10 64434789; fax: +86 10 64436781.
E-mail address: zhangjw@mail.buct.edu.cn (J. Zhang).

1385-8947/$ – see front matter © 2005 Elsevier B.V. All rights reserved.
doi:10.1016/j.cej.2005.04.010

Nomenclature

a, b	order of reaction
C_A, C_B	concentrations of reactant A and B (mol m^{-3})
C_{P0}	concentration of resultant P from instantaneous reaction at the initial time (mol m^{-3})
C_{A0}, C_{B0}	initial concentrations of reactant A and B (mol m^{-3})
C_P	the liquid concentration of P (mol m^{-3})
C_P^*	solubility of resultant P (mol m^{-3})
E_a	activation energy (kJ mol^{-1})
G	growth rate (m s^{-1})
k_A	surfacic shape factor, dimensionless
k_b	nucleation rate parameter (nb m$^{3(\alpha-1)}$ s^{-1} mol$^{-\alpha}$)
k_g	growth rate parameter (m$^{3\beta+1}$ s^{-1} mol$^{-\beta}$)
k_p	chemical reaction rate parameter
k_v	volumetric shape factor, dimensionless
k_0	pre-exponential factor
L_0	an effective size of crystal birth (m)
M_p	molecular weight of P
M_T	suspension density (kg m^{-3})
N_m	number of particles per unit volume of suspension in granulometric class m (nb m^{-3})
N_n	number of particles per unit volume of suspension in granulometric class n (nb m^{-3})
$N_{i,E}$	number of particles per unit volume in the inlet flow (nb m^{-3})
$p(l)$	the probability coefficient
Q_E	inlet volumetric flow rate (m^3 s^{-1})
Q_S	outlet volumetric flow rate (m^3 s^{-1})
r_A	the net birth rate of particles due to agglomeration per unit volume (nb m^{-1} m^{-3} s^{-1})
r_B	the net disappear rate of particles due to breakage per unit volume (nb m^{-1} m^{-3} s^{-1})
r_n	nucleation rate (nb m^{-3} s^{-1})
$r(l)$	the intrinsic rate of the agglomeration (m, n) of rank $l_{m,n}$ (nb m^{-3} s^{-1})
$R_{A,i}$	net number of particles per unit volume generated in the class i by agglomeration (nb m^{-3} s^{-1})
$R_{B,i}$	net number of particles per unit volume disappearing in the class i by breakage (nb m^{-3} s^{-1})
S_i	characteristic size of the particles of the granulometric class i, m
V_T	suspension volume (m^3)

Greek letters

α, β	kinetic parameters of crystallization
μ_j	jth moment of particle size distribution (m^j)
$\nu_{l,i}$	the overall stoichiometric coefficient of class i with respect to agglomeration of rank l
ρ_p	solid density (kg m^{-3})
$\bar{\psi}$	particle size distribution density function (nb m^{-1} m^{-3})
$\bar{\psi}_E$	particle size distribution density function of the inlet flow (nb m^{-1} m^{-3})

process, the PSD is mainly controlled by a number of simultaneously occurring phenomena within the precipitator. The main phenomena are the primary nucleation, the subsequent crystal growth as well as the agglomeration. Zukoski et al. [2] stressed that in many precipitation reactions, submicron-scale particles are formed first and then grow and sometimes may agglomerate. Liu and Nancollas [3] found that the reacting ions generate supersaturation, which becomes the driving force for both nucleation and crystal growth.

Despite its industrial importance and long history, the design as well as the operation of continuous and batch precipitators still shows some difficulties. One example is how to determine the experimental conditions for obtaining the required PSD in continuous and batch precipitators. For the solution of such operation problems as well as to gain a more thorough understanding of certain phenomena occurring in the process, mathematical modeling and numerical simulation have proven to be a valuable tool [4].

The aim of present work is to develop a new method capable of simulating the reactive precipitation process in a batch reactor. For evaluation purpose, the simulation method is applied to the production of barium sulphate through reactive precipitation under different experimental conditions. The computational results correspond with the experimental results of the precipitation of barium sulphate using stoichiometric barium chloride and sodium sulphate reagent solutions. According to the analysis of the computational results, it is found that the particle size and particle size distribution (PSD) are controlled by supersaturation and agglomeration. Some control recommendations are provided thereon.

2. Simulation fundamentals of reactive precipitation process

Present model relies on the mass and population balances and is based on the theory of precipitation. There are four main steps of reactive precipitation, i.e. chemical reaction, nucleation, growth and agglomeration. It is assumed that the experimental system is a homogeneous suspension with instantaneous mixing of the feed streams and the particles maintain their shape during the particle growth and agglomeration processes. Hence the particles can be characterized by a linear dimension L. It should be noted that present model takes no micromixing into account and is certainly not possible to reproduce all the details of the particle size distribution (PSD), however, it makes possible to check and validate the physical laws and numerical methods in cases

where micromixing effects may be neglected. An important factor of continuing interest in the operation of industrial precipitator is the particle size distribution (PSD), which is usually predicted by the population balance equation (PBE) techniques [5,6,7]. In PBE technique, the particle population balance equation needs to be solved and the population balance modeling is thus necessary for the operation, control and design of reactive precipitation vessel. In this paper, the partial differential equation that represents the particle size density function $\bar{\psi}$ is transformed into a system of ordinary differential equations by means of direct discretization of $\bar{\psi}$. The population balance equation is then solved together with mass balance and crystallization kinetics such as nucleation, crystal growth and agglomeration.

2.1. Modeling

2.1.1. General population balance

The population of the particles during the batch process is described by the density function Ψ [8]. For the sake of simplicity, it is assumed that just a linear dimension L is sufficient for the characterization of the particles due to the spherical shape of the particles under experimental observation. Hence, $\Psi(L,t)\,\mathrm{d}L$ is the number of the particles within the size range between L and $L+\mathrm{d}L$ per unit volume at time t. Then, during a time interval $\mathrm{d}t$, the balance of particles in the size interval $[L, L+\mathrm{d}L]$ can be written as follows [8]:

$$\frac{1}{V_\mathrm{T}}\frac{\partial(\bar{\psi}V_\mathrm{T})}{\partial t}+\frac{\partial(\bar{\psi}G)}{\partial L}+\frac{Q_\mathrm{S}\bar{\psi}-Q_\mathrm{E}\bar{\psi}_\mathrm{E}}{V_\mathrm{T}} = r_N\delta(L-L_0)+r_\mathrm{A}-r_\mathrm{B} \tag{1}$$

For present batch reactor, the concept of classes [9] is adopted to study the reactive precipitation.

Let L_i $(i=0,1,\ldots,N)$ be the size of particle $(\Delta L_i = L_i-(i=1,2,\ldots,N))$. L_0 is the smallest size of particles, i.e. the dimension of the nuclei; L_N is the size of the largest particles. Let $N_i(t)$ be the number of particles in the class i at time t per unit volume of suspension, then

$$N_i(t)=\int_{L_{i-1}}^{L_i}\bar{\psi}(L,t)\,\mathrm{d}L \tag{2}$$

$$R_{\mathrm{A},i}=\int_{L_{i-1}}^{L_i}r_\mathrm{A}\,\mathrm{d}L \tag{3}$$

$$R_{\mathrm{B},i}=\int_{L_{i-1}}^{L_i}r_\mathrm{B}\,\mathrm{d}L \tag{4}$$

Assuming that $\bar{\psi}$ has a constant value Φ_i at S_i ($S_i=L_i+L_{i-1}/2$) and that the value of $\bar{\psi}$ at L_i takes the arithmetic mean value of $\bar{\psi}$ at S_i and S_{i+1}, i.e.

$$N_i(t)=\phi_i(t)(L_i-L_{i-1}) \tag{5}$$

$$\bar{\psi}(L_i)=\frac{\phi_{i+1}+\phi_i}{2} \tag{6}$$

According to the above equations, we obtain the followed differential equation system:

$$\frac{\mathrm{d}N_1}{\mathrm{d}t}+\frac{1}{V_\mathrm{T}}\frac{\mathrm{d}V_\mathrm{T}}{\mathrm{d}t}N_1+\frac{Q_\mathrm{S}N_1-Q_\mathrm{E}N_{1,\mathrm{E}}}{V_\mathrm{T}}+\frac{G(L_1)}{2\Delta L_2}N_2+\frac{G(L_1)}{2\Delta L_1}N_1=r_N+R_{\mathrm{A},1}-R_{\mathrm{B},1} \tag{7}$$

$$\frac{\mathrm{d}N_i}{\mathrm{d}t}+\frac{1}{V_\mathrm{T}}\frac{\mathrm{d}V_\mathrm{T}}{\mathrm{d}t}N_i+\frac{Q_\mathrm{S}N_i-Q_\mathrm{E}N_{i,\mathrm{E}}}{V_\mathrm{T}}+\frac{G(L_i)}{2\Delta L_{i+1}}N_{i+1}+\frac{G(L_i)-G(L_{i-1})}{2\Delta L_i}N_i-\frac{G(L_{i-1})}{2\Delta L_{i-1}}N_{i-1}=R_{\mathrm{A},i}-R_{\mathrm{B},i} \tag{8}$$

$$\frac{\mathrm{d}N_N}{\mathrm{d}t}+\frac{1}{V_\mathrm{T}}\frac{\mathrm{d}V_\mathrm{T}}{\mathrm{d}t}N_N+\frac{Q_\mathrm{S}N_N-Q_\mathrm{E}N_{N,\mathrm{E}}}{V_\mathrm{T}}+\frac{G(L_N)-G(L_{N-1})}{2\Delta L_N}N_N-\frac{G(L_{N-1})}{2\Delta L_{N-1}}N_{N-1}=R_{\mathrm{A},N}-R_{\mathrm{B},N} \tag{9}$$

2.1.2. Further assumptions for present model

To obtain the model equations for the present precipitation system, the following assumptions are adopted here:

(1) The suspension is perfectly mixed from a macroscale view.
(2) There are no noticeable micromixing effects.
(3) The solubility of crystalline is constant.
(4) The suspension volume is constant during the crystallization process, $\mathrm{d}V_\mathrm{T}/\mathrm{d}t=0$.
(5) Crystal growth rate is independent of particle size, i.e. the crystal growth obeys McCabe Law.
(6) No breakage occurs and Ostwald ripening has no noticeable influence.

In the model, it is further considered that $\Delta L_i=\Delta L_{i+1}$ $(i=1,2,\ldots,\mathrm{N}-1)$.

According to the above assumptions and the experimental conditions, a system of differential governing equations is obtained as follows:

$$\begin{aligned}&\frac{\mathrm{d}N_1}{\mathrm{d}t}+\frac{G}{2\Delta L}(N_2+N_1)=r_N+R_{\mathrm{A},1},\\&\frac{\mathrm{d}N_i}{\mathrm{d}t}+\frac{G}{2\Delta L}(N_{i+1}-N_{i-1})=R_{\mathrm{A},i},\\&\frac{\mathrm{d}N_N}{\mathrm{d}t}-\frac{G}{2\Delta L}N_{N-1}=R_{\mathrm{A},N},\quad i=2,3,\cdots n-1\end{aligned} \tag{10}$$

with the initial condition:

$$t=0,\ N(L,0)=0 \tag{11}$$

and boundary condition:

$$L = L_0,\ N(L_0, t) = \frac{r_N(t)}{G(t)} \tag{12}$$

2.1.3. Description of the chemical reaction rate

During the reaction precipitation process, two or more components react chemically, resulting in the formation of a new product. Considering a chemical reaction between two ionic solutions A and B with the respective concentration C_A and C_B leading to a solid P and an ionic solutions Q in a batch reactor

$$aA + bB \rightarrow pP \downarrow + qQ$$

Reaction rate equation:

$$\frac{dC_P}{dt} = k_0 \exp\left(-\frac{E_a}{RT}\right) C_A^a C_B^b = k_p C_A^a C_B^b \tag{13}$$

Generally, fast chemical reaction or instantaneous chemical reaction is chosen in preparing ultrafine particles through reactive precipitation process. For instantaneous chemical reaction, $k_p \rightarrow \infty$, if the influence of mixing is not considered, the reactive precipitation process is controlled by crystallization. For the case of an instantaneous chemical reaction (e.g. the formation of Barium Sulphate by reaction precipitation as used in the following experiment of present paper), the reaction instantaneously occurred and finished when the two reactants contact with each other. Hence, at the initial time, if C_{A0}:$C_{B0} = a$:b (C_{A0}, C_{B0} are the initial concentrations of reactant A and B), one obtains:

$$C_P = C_{P0} = \frac{p}{a} C_{A0}$$

2.1.4. Description of the nucleation process

During the precipitation process, new crystals are created by nucleation events. The rate of nucleation plays an important role in the particle size distribution (PSD) of precipitation products. In precipitation process, when the stirred speed is constant, the rate of nucleation can be presented by the empirical expression [1]:

$$r_N = k_b (C_P - C_P^*)^\alpha \tag{14}$$

2.1.5. Description of the crystal growth

Nuclei are formed during the first period of precipitation and grow by the advancement of their individual faces. In precipitation process, the crystal growth rate is a crucial parameter since it determines the final specific properties of crystals such as the particle morphology and the final particle size distribution (PSD). For the case the growth independent of particle size, when the stirred speed is constant, the growth rate can be expressed as [10]:

$$G = k_g (C_P - C_P^*)^\beta \tag{15}$$

2.1.6. Description of the particle agglomeration

Apparent agglomeration between the particles was observed in the present experiments and it must be taken into consideration for modeling. While nucleation and crystal growth are normally considered to be dominant in the process of particle formation, some secondary events such as particle agglomeration can also occur in the precipitation process of preparing ultrafine particles. It is, when it arises, largely responsible for the final product properties, such as PSD, surface area or filterability. In general, the agglomeration process in a precipitation is comprehensively described by two consecutive steps [11]: first, the particles collide with each other and then adhere together to form an aggregate; and then, the aggregate become the concrete agglomerate by the molecular growth process of the precipitation. In this paper, the agglomeration process is considered as a chemical reaction between the particles in different classes. For N granulometric classes, there may occur $N(N+1)/2$ different agglomerations between any two particles. A symbol of (m, n) is applied to represent the agglomeration of a particle in the class m with a particle in the class n by assuming that $n \geq m$. It is possible to arrange the different agglomerations in such a way that $l_{m,n}$ being the rank of the agglomeration (m, n)

$$l_{m,n} = N(m-1) - \frac{m(m-1)}{2} + n \tag{16}$$

$$l_{\max} = \frac{N(N+1)}{2} \tag{17}$$

As a chemical reaction does, agglomeration preserves the total mass of particles. For the agglomeration of a particles of class m with b particles of class n to form c particles of class q, the following relationship exists:

$$aS_m^3 + bS_n^3 = cS_q^3 \tag{18}$$

If $a = b = 1$, then $c = (S_m^3 + S_n^3)/S_q^3$.

Considering a particular class i, the agglomeration of rank $l_{m,n}$ will affect this class only in three case:

$i = m$ with stoichiometric coefficient -1,
$i = n$ with stoichiometric coefficient -1,
$i = q$ with stoichiometric coefficient $v = (S_m^3 + S_n^3)/S_q^3$.

Therefore, the overall stoichiometric coefficient of class i with respect to agglomeration of rank l is

$$v_{l,i} = \left[\frac{S_m^3 + S_n^3}{S_q^3}\right] \delta_{i,q} - (\delta_{i,m} + \delta_{i,n}) \tag{19}$$

where $\delta_{ij} = 1$ if $i = j$ and $\delta_{ij} = 0$ if $i \neq j$.

The net rate of particle production by agglomeration in the class i is calculated from $v_{l,i}$ and the intrinsic rate of the agglomeration of rank l as for a set of chemical reactions:

$$R_{A,i} = \sum_{l=1}^{l_{\max}} v_{l,i}\, p(l)\, r(l) \tag{20}$$

where $p(l)$ is the probability coefficient which stands for the assumption that agglomeration cannot produce particles bigger than those of class N:

- If $S_q > S_N$, then $p(l) = 0$.
- If $S_q \leq S_N$, then $p(l) = 1$.

The intrinsic rate of the agglomeration (m, n) of rank $l_{m,n}$ is expressed by the empirical law:

$$r = \bar{K}\Delta C^j N_m N_n \tag{21}$$

2.1.7. Moment analysis

The moments of the distribution represent the averaged and overall properties of the solid phase, and this approach is sufficient to provide useful information for engineering and design purposes.

The ith moment of the distribution is defined as:

$$\mu_i = \int_0^\infty \psi L^i \, \mathrm{d}L, \quad i = 0, 1, 2, \ldots \tag{22}$$

In industrial production, the averaged particle size and the variance are the main concerns.

The area-based characteristic size of the crystals and variance can be expressed as:

$$d_{32} = \frac{\mu_3}{\mu_2} \tag{23}$$

$$\sigma_{32} = \sqrt{\left(\frac{\mu_4}{\mu_2}\right) - \left(\frac{\mu_3}{\mu_2}\right)^2} \tag{24}$$

The volume-based characteristic size of the crystals and variance can be expressed as:

$$d_{43} = \frac{\mu_4}{\mu_3} \tag{25}$$

$$\sigma_{43} = \sqrt{\left(\frac{\mu_5}{\mu_3}\right) - \left(\frac{\mu_4}{\mu_3}\right)^2} \tag{26}$$

Suspension density:

$$M_\mathrm{T} = \rho k_\mathrm{v} \mu_3 \tag{27}$$

Surface area of crystal:

$$A_\mathrm{T} = k_\mathrm{A} \mu_2 \tag{28}$$

2.1.8. Mass balance

The supersaturation degree can be estimated from the balance between the production of solute due to chemical reaction and its consumption due to both nucleation and crystal growth, as follows:

$$\frac{\mathrm{d}C_\mathrm{P}}{\mathrm{d}t} = k_\mathrm{p} C_\mathrm{A}^a C_\mathrm{B}^b - \frac{\rho_\mathrm{p} k_\mathrm{v}}{M_\mathrm{p}} 3G\mu_2 - \frac{\rho_\mathrm{p} k_\mathrm{v}}{M_\mathrm{p}} r_N L_0^3 \tag{29}$$

For the system of instantaneous chemical reaction, Eq. (29) can be simplified as:

$$\frac{\mathrm{d}C_\mathrm{P}}{\mathrm{d}t} = -\frac{\rho_\mathrm{p} k_\mathrm{v}}{M_\mathrm{p}} 3G\mu_2 - \frac{\rho_\mathrm{p} k_\mathrm{v}}{M_\mathrm{p}} r_N L_0^3 \tag{30}$$

with $t = 0$, $C_\mathrm{P} = C_{\mathrm{P}0}$.

2.2. Simulation procedure

Usually, the population balance can be calculated by moment method. But the particle size distribution cannot be obtained directly according to the moment method. In this paper, the population balance equation is calculated by the discretization method [8] in which the equations are transformed into a system of ordinary differential equations. The system of ordinary differential equations can be solved by Runge–Kutta method.

The structure of simulation procedure is illustrated in Fig. 1.

3. Experiments

It is crucial to validate the model for application. Usually, this is based on the published nucleation and crystal growth kinetic expressions. In this paper, barium sulphate synthesized through the reaction between barium chloride and sodium sulphate is taken as the work system since this system has been widely investigated experimentally and reported in the literature with sufficient kinetic parameters. This reactive precipitation process is a typical precipitation process of fast chemical reaction and fast nucleation

$$\mathrm{BaCl_2 + NaSO_4 \rightarrow BaSO_4 \downarrow + NaCl_2}$$

3.1. Experimental process

The experiment of reactive precipitation was conducted as follows: in a batch experiment, precipitation was initiated by quickly adding (less than 3 s) barium chloride solution to sodium sulphate solution in a perfectly thermostat well-mixed precipitator. The order of addition of reactants was also reversed in some experiments. The initial concentration ratio $R_0 = C^0_\mathrm{Ba}/C^0_{\mathrm{SO_4}}$ conformed to stoichiometrical condition. During the precipitation process, some suspension samples were withdrawn from the precipitator at different time intervals. The suspension samples were added to the dispersant, and then supersonic shaker dispersed the suspension samples. Transmission electron microscope micrographs of crystals were taken in order to observe agglomeration phenomenon and estimate their shape factors. The particle was sampled and the particle size distribution (PSD) was measured by a MALVERN ZETASIZER 3000HS analyzer.

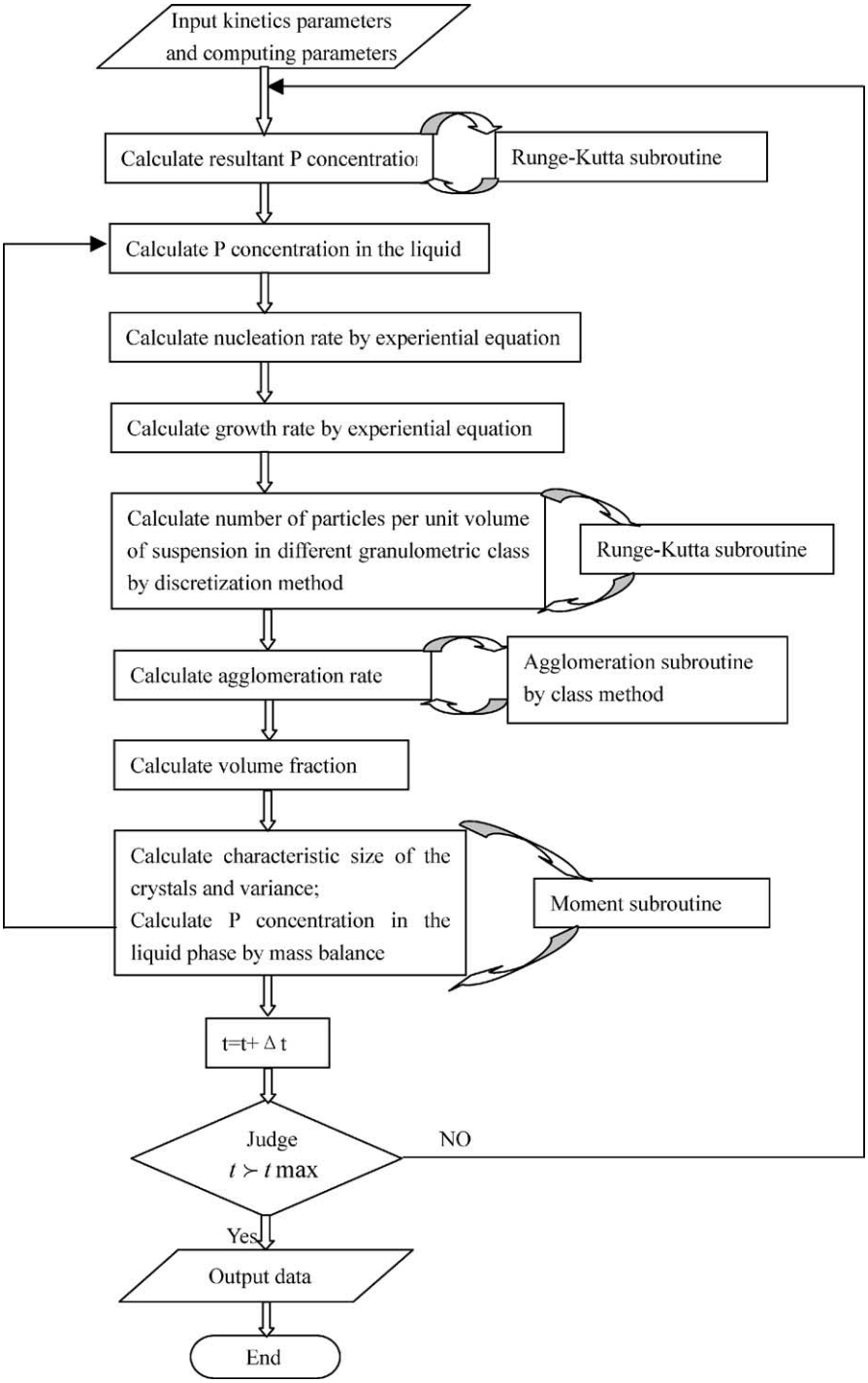

Fig. 1. The structure of simulation procedure.

3.2. The comparison between experimental and computational results

The observation of the particles by transmission electron microscope (TEM) micrographs in Fig. 2 shows that the particles under the experimental conditions are obviously agglomerated and the agglomeration has an important influence on the particle size and particle size distribution (PSD).

Model simulation is carried out for validation purpose. The parameters used in the model are as follows.

The parameters for nucleation rate, growth rate and crystallization kinetic are derived from the literature [12] as follows:

$$k_b = 6.0 \times 10^{12}\,\mathrm{nb\,m^{2.325}\,s^{-1}\,mol^{-1.775}}, \quad \alpha = 1.775$$

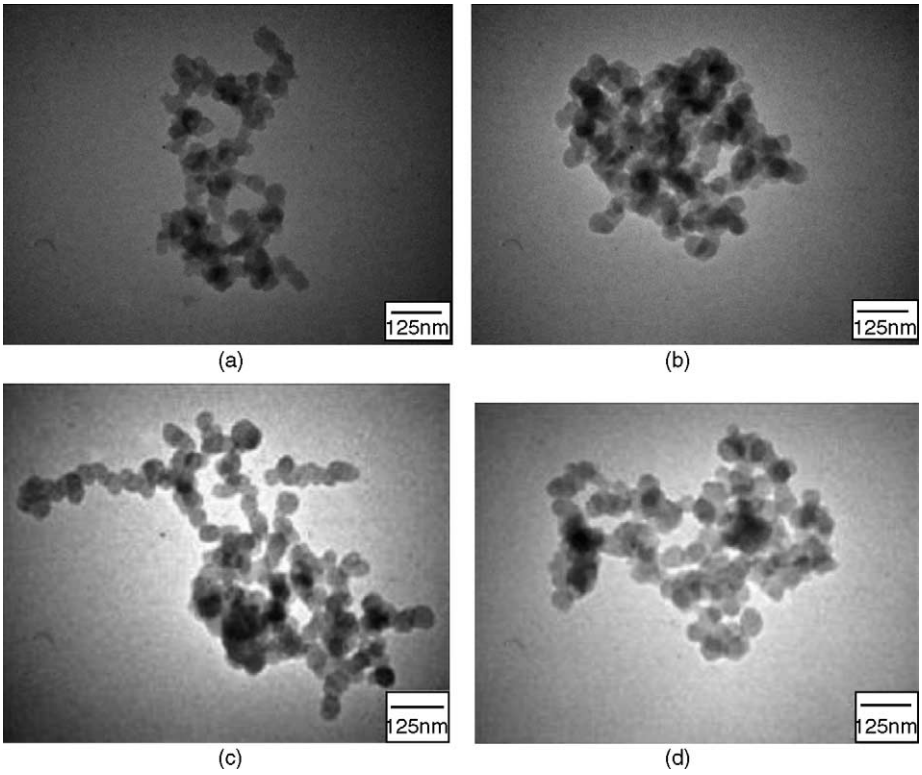

Fig. 2. TEM micrographs of particle products.

$k_g = 2.3 \times 10^{-10}\,m^4\,s^{-1}\,mol^{-1}, \quad \beta = 1.0$

According to the experimental observation, the shape of particle is spheric. We can get volumetric shape factor and surfacial shape factor of sphere:

$k_v = 0.523, \quad k_A = 3.14$

$\bar{K}$ and j are the experimental fitting parameters and are determined by experiment

$\bar{K} = 1.0 \times 10^{-21}$

$j = 1.0$.

Fig. 3 depicts the comparison between experimental results and computational results. It is found that the particle size distribution trend of computational results is identical to that of experimental results, and the biggest error of PSD is about 22% occurring at 650 nm. It should be mentioned that for comparison purpose, careful options of integration time steps of 0.01, 0.05, 0.1, 0.2 s are carried out and the computational results show the irrelevance to the time step. In this paper, a time step of 0.1 s is used for all modeling for saving calculation time.

4. Analysis of simulated results

In this section, present model is applied to investigate the effects of supersaturation degree and agglomeration on particle size and particle size distribution and their evolutions during the reactive precipitation process.

4.1. The evolution of desupersaturation

The desupersaturation curves are presented in Fig. 4. During the first moments after mixing began there seems no apparent consumption occurring although in fact primary nucleation takes place and results in very small nuclei. When the total particle surface becomes large enough, barium sulphate in the liquid phase is consumed by particle growth. If barium sulphate concentration in the liquid phase is sufficiently close to the solubility, the concentration drop

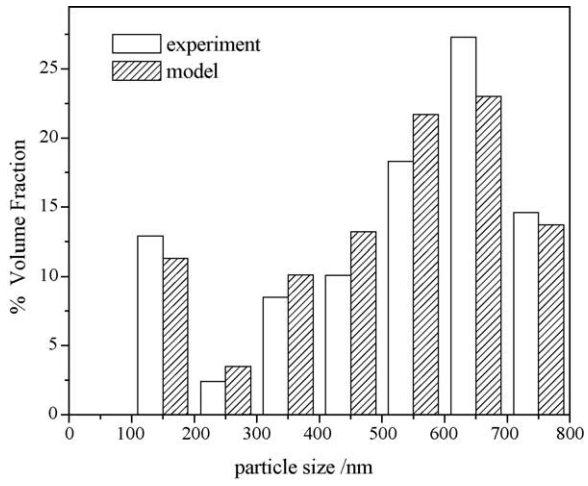

Fig. 3. Comparison between experimental results and computational results ($C_{inlet} = 10\,mol\,m^{-3}$; $t = 93\,s$; $T = 25\,^{\circ}C$; stirred speed: 600 rpm).

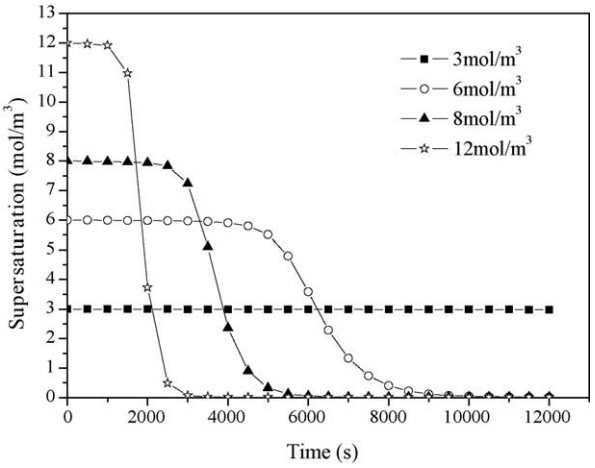

Fig. 4. Desupersaturation curves against time at different initial concentrations.

stop. In the event of the initial concentrations of the reactants being increased, that is, the barium sulphate supersaturation being increased, the first stage of the crystallization where primary nucleation predominated is shortened. In case the initial feed reactant concentrations are 3 mol m^{-3}, the drop of barium sulphate concentration against time is hardly registered and this run cannot be exploited.

4.2. The evolution of the volume-based characteristic size of the particles

Fig. 5 illustrates that the volume-based characteristic size of the particles increases continuously with time. The fastest increase is registered for the highest initial concentrations of the reactants, but the final size of particles is in the range 1.2–1.4 μm. The higher the initial concentrations of the reactants are, the bigger the size of particles becomes. However, the overall influence of the initial concentrations of the reactants remains moderate.

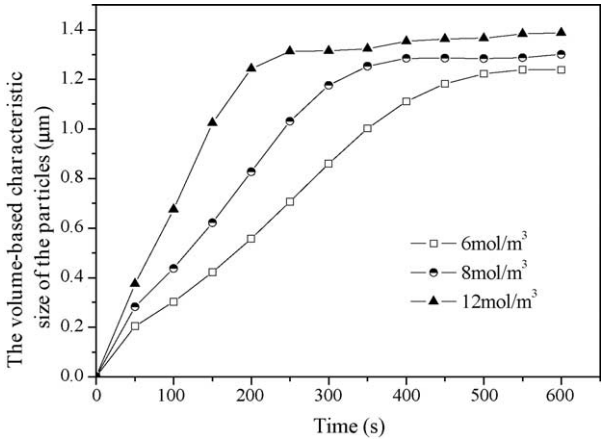

Fig. 5. The volume-based characteristic size of the particles as a function of time at different initial concentrations.

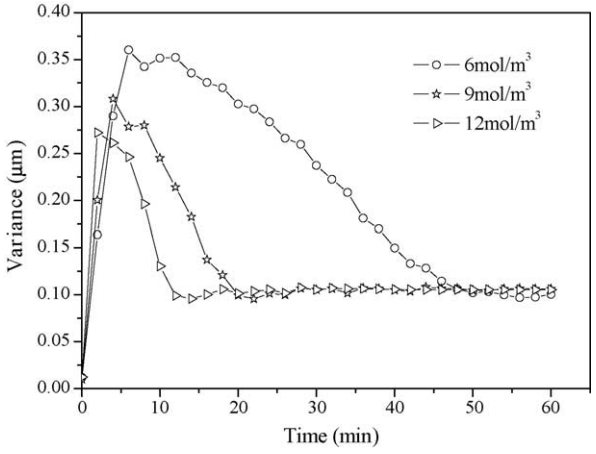

Fig. 6. The variance of volume-based characteristic size of the particles as a function of time at different initial concentrations.

4.3. The variance of the particle volume-based characteristic size

The curves of the variance of volume-based characteristic size of the particles at different initial concentrations of the reactants are depicted in Fig. 6. Evolution of the variance of the volume-based characteristic size of the particles against time resembles a normal distribution and the final values all come to 0.1 μm. The distributions become narrow and the biggest variance value drops with increasing the initial concentrations of reactants, accordingly, the time at which the biggest variance value occurs is shortened.

4.4. The influence of the precipitation time

In the study range of this paper, it is found that the longer the time, the wider the particle size distribution (PSD), and the bigger the average size of particles for the same initial concentrations of reactants. It is also shown in Fig. 7 that, during the reactive precipitation process, agglomeration

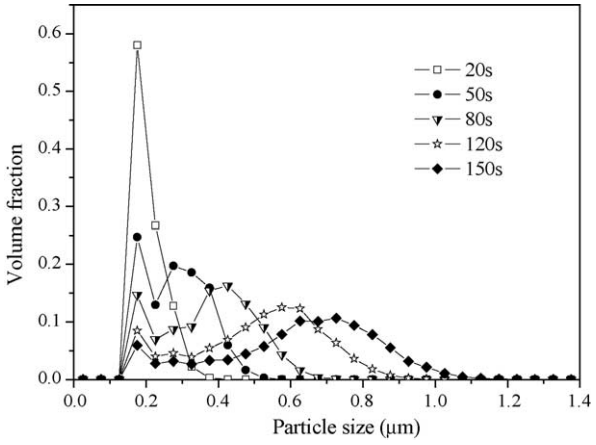

Fig. 7. Particles size distributions at different time (C_{inlet} = 8 mol m^{-3}).

phenomenon occurs in a time range. The PSD widen and the average size of the particles become larger with the time increasing. No agglomeration is detected at 20 s, and the PSD appears a shape of normal distribution, but the agglomeration occurs at 50 s, and the curve of PSD has two peaks. According to the observation and analysis of the computational results, it is obvious that the time of reactive precipitation has an important influence on both the particle size and the particle size distribution (PSD).

4.5. The influence of supersaturation degree

The nucleation rate extremely depends on the supersaturation degree. A small change of supersaturation will lead to extreme change of nucleation rate, which is the fundamental difficulty for controlling precipitation reaction in industrial production. Simultaneously, the supersaturation degree in a precipitator often markedly affects the PSD of the product. According to the computational results presented in this paper, if the initial concentrations of the reactants are high, the initial concentration of the product is also high, but the solubility is very low, the resulted high supersaturation leads to a wide PSD range. However, it may be different in different supersaturation ranges. In general, when supersaturation is below a constant value, the PSD widening and the mean characteristic size of the particles increase with increasing supersaturation. When, however, supersaturation is above the constant value, the PSD narrows and the mean characteristic size of particles decreases with increasing supersaturation. This is due to different crystallization kinetics parameters.

To obtain the special size of the particles and PSD, it is essential to control the appropriate supersaturation. Fig. 8 shows PSD of different initial concentrations of reactants at 90 s. In addition, it should be noted that the curves of PSD of particles have two peaks, which is the basic characteristic of PSD of particles prepared by reactive precipitation.

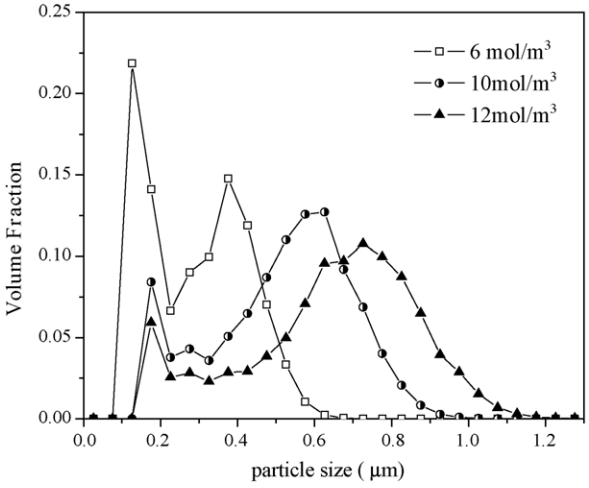

Fig. 8. Particles size distributions at different initial concentrations (t = 90 s).

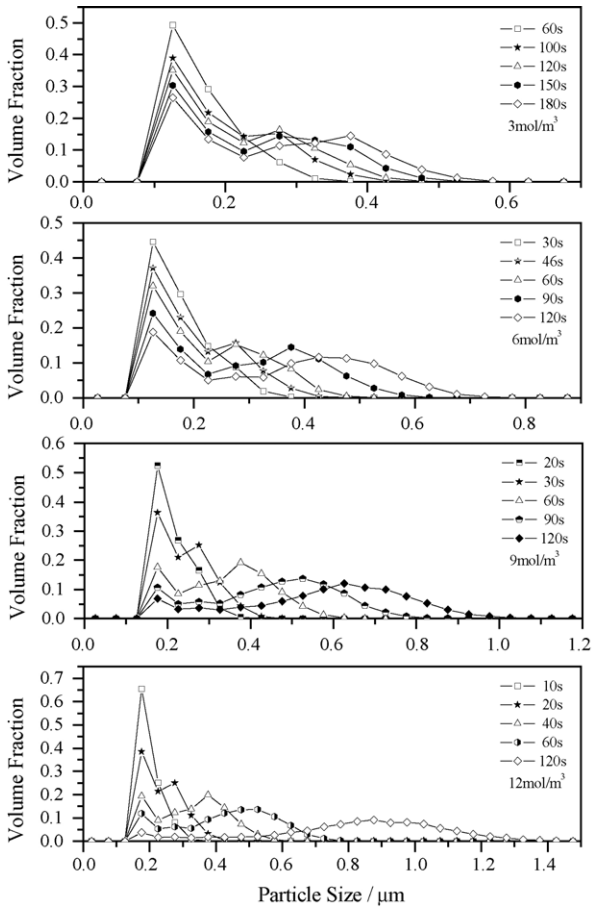

Fig. 9. Particles size distributions at different time for different initial concentration.

The initial concentrations of barium chloride and sodium sulphate in the feed strongly influence the degree of agglomeration. The degree of agglomeration is enhanced with increasing initial concentrations of reactants. The explanation is that both supersaturation and particle number densities N_m and N_n are increased in that case. When the initial concentrations of reactants are increased, accordingly, the resultant supersaturation is increased, the degree of agglomeration is strengthened and the time that the second peak appears is shortened. Fig. 9 shows the higher the supersaturation, the shorter the time that the second peak appears.

4.6. The influence of agglomeration

The method of classes proposed by Marchal and David [8] is used to introduce agglomeration in the model. According to the calculated results, it is found that, during the reactive precipitation process, there is a time range, in which two peaks appear along the PSD curves, that is, the PSD curves take the shape of 'S'. That corresponds with the results of the present experiment and that from literatures [13]. The main conclusion from this model is that agglomeration cannot be considered as a size-independent phenomenon. There existed

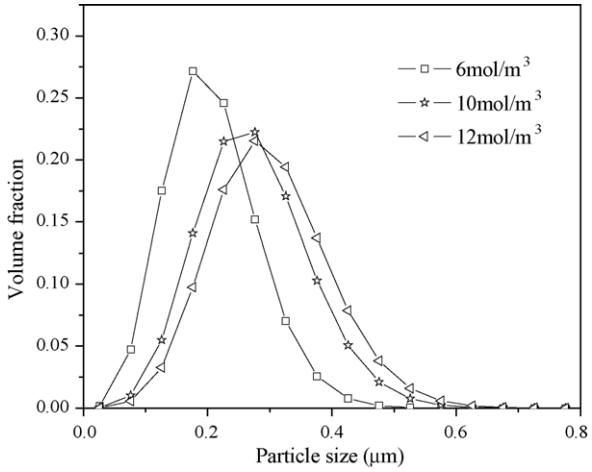

Fig. 10. Calculated particles size distributions at different initial concentrations (t = 120 s, no agglomeration considered).

a size range where agglomeration may occur and the ratio of the characteristic sizes of agglomerating particles plays a major role in the process. Small particles stick more easily to larger ones than particles of equal size do. As can be seen from Figs. 7–9, the agglomeration phenomenon appears to follow the following rules:

(1) The second peak gradually moves to the direction of relative bigger particle size at the same initial concentrations of reactants with the time increasing; accordingly, the disparity of particle size between the first peak and the second peak enlarges.
(2) The disparity of the particle size between the first peak and the second peak enlarges with the increasing supersaturation, at the same time; accordingly, the peak value drops.
(3) At the same initial concentrations of reactants, all the first peaks of the curves of PSD at different time appear at a special particle size, i.e. all the first peaks of the curves of PSD at different time appear at 170 nm in Fig. 7.

According to the above analysis, in order to control PSD of ultrafine particles, attention should be paid to reduce the influence of agglomeration between the smaller particles and the bigger particles and control the appropriate the precipitation time and supersaturation degree.

Besides, if we do not consider the agglomeration in the model, the PSD is normal distribution. Fig. 10 shows the calculated particle size distributions at different initial concentrations without considering the agglomeration between the particles.

5. Conclusions

(1) Based on the population and mass balances of the reactive precipitation process, a numerical model including reaction, nucleation, growth and agglomeration is developed to predict particle size distribution (PSD) in reactive precipitation process. Moreover, the construction of this model is simple and the model is apt to calculation.
(2) During the reactive precipitation process, agglomeration phenomenon is obviously observed by experimental study. By making use of the model, the agglomeration is studied and the correspondence between the computational results and the experimental results is fairly satisfactory.
(3) According to the model results, the evolution rules of supersaturation, volume-based characteristic size and variance of volume-based characteristic size of the particles with time are found. On a further aspect, the model results show supersaturation and agglomeration have important influences on the particle size and particle size distribution (PSD) and the evolution trend of PSD with time is provided. In this paper, the disciplinarian of influences of these factors and the method for controlling particle size distribution are presented for reactive precipitation process.

Acknowledgements

The authors acknowledge the financial support from National Science Foundation of China (No. 20236020) and the Doctoral Program Foundation of Institutions of Higher Education of China (No. 20010010004) that allows the authors to accomplish the research presented herein. Great thanks also would be made to Dr. Zhigang Shen for his contributions to this work.

References

[1] A.D. Randolph, M.A. Larson, Theory of Particulate Processes, Academic Press, New York, 1988.
[2] C.F. Zukoski, D.F. Rosenbaum, P.C. Zamora, Aggregation in precipitation reactions: stability reactions – stability of primary particles, Trans. Inst. Chem. Eng. Part A 74 (1996) 723–731.
[3] S.T. Liu, G.H. Nancollas, Scanning electron microscopic and kinetic studies of the crystallization and dissolution of barium sulphate crystals, J. Cryst. Growth 33 (1976) 11–20.
[4] R. Miller, Witkowski, Model identification and control of solution crystallization processes, Ind. Eng. Chem. Res. 32 (1993) 1275–1296.
[5] J. Benjamin, McCoy, A new population balance model or crystal size distributions: reversible, size-dependent growth and dissolution, J. Colloid Interf. Sci. 240 (2001) 139–149.
[6] S. Tsantilis, H.K. Kammler, S.E. Pratsinis, Population balance modeling of flame synthesis of titania nanoparticles, Chem. Eng. Sci. 57 (2002) 2139–2156.
[7] D. Verkoeijen, A.G. Pouw, M.H. Meesters, G.B. Scarlett, Population balances for particulate processes — a volume approach, Chem. Eng. Sci. 57 (2002) 2287–2303.
[8] P. Marchal, R. David, Crystallization and precipitation engineering. I. An efficient method for solving population balance in crystallization with agglomeration, Chem. Eng. Sci. 43 (1988) 59–67.
[9] R. David, P. Marchal, J.P. Klein, J. Villermaux, Crystallization and precipitation engineering. III. A discrete formulation of the agglomeration rate of crystals in a crystallization process, Chem. Eng. Sci. 46 (1990) 205–213.

[10] N.S. Tavare, J. Garside, Simultaneous estimation of crystal nucleation and growth kinetics from batch experiments, Chem. Eng. Res. Des. 64 (1986) 109–118.
[11] J.C. Macy, M. Cournil, Using a turbidimetric method to study the kinetics of agglomeration of potassium sulfate in a liquid medium, Chem. Eng. Sci. 46 (1991) 693–701.
[12] M. Aoun, E. Plasari, R. David, J. Villermaux, A simultaneous determination of nucleation and growth rates from batch spontaneous precipitation, Chem. Eng. Sci. 54 (1999) 1161–1180.
[13] J.A. Dirksen, Fundamentals of crystallization: kinetic effects on particle size distributions and morphology, Chem. Eng. Sci. 46 (1991) 2389–2427.